J. Am. Ceram. Soc., 95 [2] 651–657 (2012)
DOI: 10.1111/j.1551-2916.2011.04803.x

journal

Structure and the Electrical Properties of $Pb(Zr,Ti)O_3$ – Zirconia Composites

Andreja Benčan,[‡,†] Barbara Malič,[‡,*] Silvo Drnovšek,[‡] Jenny Tellier,[‡] Tadej Rojac,[‡] Jernej Pavlič,[‡] Marija Kosec,[‡,*] Kyle G. Webber,[§] Jürgen Rödel,[§,**] and Dragan Damjanovič[¶,*]

[‡]Jožef Stefan Institute, 1000, Ljubljana, Slovenia

[§]Institute of Materials Science, Technische Universität Darmstadt, 64287, Darmstadt, Germany

[¶]Ceramics Laboratory, Swiss Federal Institute of Technology, EPFL, 1015, Lausanne, Switzerland

In this work, the effect of introducing tetragonal yttria-stabilized zirconia (TZ) particles in soft $[Pb_{0.98}Ba_{0.01}][(Zr_{0.53}Ti_{0.47})_{0.98}Nb_{0.02}]O_3$ (PZT) was investigated. Both microstructure and electrical properties of the PZT–xTZ (x = 0, 2, 5, 10, 20 vol%) composites were studied and correlated. The addition of zirconia hinders the matrix grain growth, resulting in smaller grains. According to X-ray diffraction analysis, zirconia containing composites have a higher rhombohedral-to-tetragonal phase ratio, in addition to lower dielectric and piezoelectric properties, in comparison to pure PZT. Electrical properties, in terms of strain– and polarization–electric field hysteresis curves, are presented and correlated with the observed phase compositions and microstructures. The extrinsic contribution to the piezoelectric properties in PZT and PZT–xTZ was studied by measuring the frequency and the stress field amplitude dependences of the piezoelectric d_{33} coefficient.

I. Introduction

Ceramic piezoelectric materials based on the lead zirconate titanate solid solution with compositions near the morphotropic phase boundary (MPB) are commercially important due to their excellent electromechanical properties.[1] Unfortunately, similarly to that of nonpiezoelectric ceramics, such as aluminum oxide, these materials are brittle, which presents severe limitations on some applications, for example, diesel fuel injectors and bending actuators.[2] Various toughening mechanisms, such as the addition of SiC whiskers,[3] ZnO nanowhiskers,[4] or various binary oxide particles, such as ZrO_2,[5–7] Al_2O_3, MgO,[6] or $Bi_4Ti_3O_{12}$,[8] have been suggested to improve the mechanical properties of lead zirconate titanate ceramics.

Malič *et al.*[5] studied the effects of the addition of monoclinic zirconia (m-ZrO_2) to $Pb_{0.94}Sr_{0.06}(Ti_{0.48}Zr_{0.52})O_3$ ceramics. The authors observed an increase in the strength of the composite with up to 8 vol% of m-ZrO_2. This was due to an increase in microcracking generated by the spontaneous transformation of zirconia particles from the high-temperature tetragonal phase to the monoclinic phase during cooling from the sintering temperature. The strength of the composite was 140 MPa compared to 100 MPa for pure ceramics. Tajima *et al.*[6] compared the effects of Al_2O_3, MgO, and m-ZrO_2 additives on the microstructure and mechanical properties of $Pb(Zr_{0.52}Ti_{0.48})O_3$ ceramics. While the addition of 0.1–1.0 vol% Al_2O_3 and 0.1 vol% MgO reduced the matrix grain size and improved the fracture strength of the ceramics by ~70%, the addition of 1 vol% m-ZrO_2 had little effect on the grain size and the mechanical properties.

Recently, an improvement of the strength and fracture toughness (as measured by three-point bending method and single-edge notched beam test) with slightly decreased piezoelectric properties was achieved for $Pb_{0.99}(Zr_{0.58}Ti_{0.42})_{0.98}Nb_{0.02}O_3$–$ZrO_2$ composites prepared by the precipitation method.[7] In the composites, both monoclinic and tetragonal ZrO_2 crystal phases were found to be present. The authors ascribed the improvement of the fracture strength (94 MPa compared to 78 MPa for pure ceramics) and fracture toughness (2.27 $MPam^{1/2}$ compared to 1.45 $MPam^{1/2}$ for pure ceramics) of the composites with 4 mol% of ZrO_2 to the different toughening mechanisms, that is, microcracking, nanoparticle dispersion and transformation toughening. Note that the latter is a mechanism used extensively to toughen electroinactive ceramics, such as zirconia or alumina.[9,10]

In this work, $[Pb_{0.98}Ba_{0.01}][(Zr_{0.53}Ti_{0.47})_{0.98}Nb_{0.02}]O_3$ (PZT) with the addition of a second phase of tetragonal yttria-stabilized zirconia particles is investigated. The microstructural, electrical, and piezoelectric properties of PZT with varying concentrations (0, 2, 5, 10, and 20 vol%) of yttria-stabilized zirconia particles (TZ) were studied. Fracture behavior has also been studied, showing enhanced fracture toughness with the inclusion of yttria-stabilized zirconia particles, and will be published separately. Interrelated factors that influence the electrical properties of the composites, such as PZT matrix grain size and phase composition (rhombohedral-to-tetragonal phase ratio) are presented and discussed.

II. Materials and Chracterization Methods

The powder mixtures with the nominal composition $[Pb_{0.98}Ba_{0.01}][(Zr_{0.53}Ti_{0.47})_{0.98}Nb_{0.02}]O_3$ were prepared by mixed-oxide method using PbO (99.9% purity; Sigma, Steinheim, Germany), TiO_2 (99.8% purity; Alfa, Karlsruhe, Germany), ZrO_2 (TZO; Tosoh, Yamaguchi, Japan), Nb_2O_5 (99.9% purity; Sigma), and $BaCO_3$ (99.8% purity; Alfa) as precursors. Powder mixtures were homogenized in isopropyl alcohol (C_3H_7OH) in a planetary mill and calcined twice at 900°C/1 h, with 5°C/min of heating/cooling rate, with milling after each calcination. As shown in Fig. 1(a), after the second calcination at 900°C for 1 h, the powder mixtures were composed of $PbZrO_3$, $PbTiO_3$, tetragonal and rhombohedral lead zirconate titanate solid solutions, and a PbO-rich phase. According to the granulometric analysis (Microtrac S3500 Series Particle Size Analyzer, Montgomeryville, PA), the medium grain size, calculated from the area distribution, was 0.39 μm. The particle size distribution of the powder mixture is shown in Fig. 1(b).

J. L. Jones—contributing editor

Manuscript No. 29716. Received May 11, 2011; approved July 18, 2011.
This project was supported by the European Union under the Seventh Framework project HIgh-PERformance Piezoelectric Actuators—HIPERAct.
*Member, The American Ceramic Society.
**Fellow, The American Ceramic Society.
[†]Author to whom correspondence should be addressed. e-mail: andreja.bencan@ijs.si

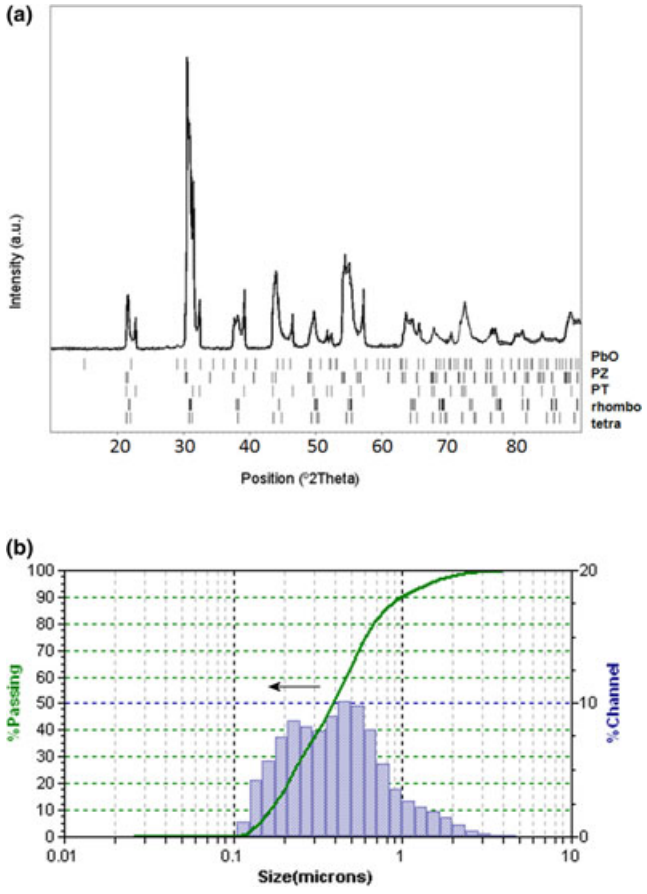

Fig. 1. XRD pattern of PZT after the second calcination at 900°C for 1 h. Calculated positions of hkl reflections for PbO (PDF-ICDD, 05-0570), $PbZrO_3$ (PDF-ICDD: 35-0739), $PbTiO_3$ (PDF-ICDD:06-0452), tetragonal PZT $(Pb(Zr_{0.52}Ti_{0.48})O_3$, PDF-ICDD: 33-0784), and rhombohedral PZT $(Pb(Zr_{0.58}Ti_{0.42})0_3$, PDF-ICDD:73-2022) are added (a). The particle size distribution of the powder mixture is shown in (b).

Various concentrations (2, 5, 10, or 20 vol%) of as-received tetragonal stabilized zirconia with 3 mol% Y_2O_3 (TZ3Y; Tosoh, denoted as TZ) was added to the prepared powder mixture. The XRD analysis showed that as-received TZ powder was a mixture of tetragonal and monoclinic phases with 81 wt% of tetragonal phase. The TZ powder was composed of grains ~50 nm in size (Fig. 2).

The PZT–xTZ (x = 2, 5, 10, 20 vol%) powder mixtures were additionally homogenized in an attrition mill, pressed into pellets, and sintered at 1275°C for 2 h with the heating/cooling rate 5°C/min. To prevent the PbO sublimation during sintering, the packing powder of the same composition was used. The densities of the sintered pellets were determined by the Archimedes' method. Theoretical densities of composites (TD) were calculated according to Eq. (1):

$$TD_{composite} = TD_{ZrO_2} v_{ZrO_2} + TD_{PZT} v_{PZT} \quad (1)$$

where v is the volume fraction of the corresponding component. The values used for TD of ZrO_2 and of PZT were 5.83 kg/m^3 [11] and 8.00 kg/m^3 [12] respectively.

X-ray powder diffraction was performed using PANalytical X'Pert PRO diffractometer with Cu$K\alpha_1$ radiation (Almelo, the Netherlands). For the XRD analysis of the sintered samples, the pellets were crushed into powders. The data were collected in the 2θ range from 10° to 90° with a step of 0.034°/100 s. Rietveld refinements were performed to estimate the phase ratio and the unit cell volume of the phases. The refinements were made using the Jana2006 program.[13] For the refinement, the tetragonal (ICSD 90699, SG: P4mm) and rhombohedral (ICSD 90700, SG:R3mH) crystal structures of PZT were used. The input parameters, such as space group, cell parameters, and atomic positions, were based on refined structures available in the ICSD database. The refinement was done on the background parameters (Lorentz polynomial), unit cell parameters, zero position shift, profile parameters (pseudo-Voigt function), and phase ratio. The atomic positions were kept constant.

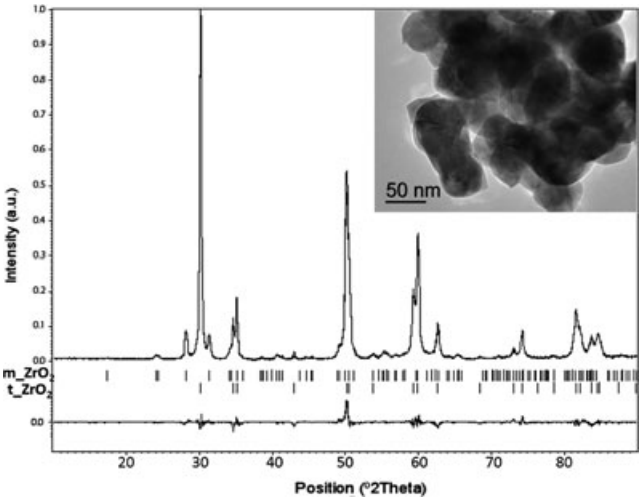

Fig. 2. Final observed, calculated (hkl reflections for tetragonal ZrO_2 [ICSD 9993] and monoclinic ZrO_2 [ICSD 57157]) and difference plots for the XRD Rietveld refinement of as-received TZ powder. The reliability factors [$R_{w(all)}$] were 3.07% for tetragonal and 2.54% for monoclinic phase. The goodness of fit (GOF) was 1.30. Inset shows the TEM micrograph of TZ powder.

The fracture surfaces, as well as the polished and thermally etched surfaces, were analyzed using a field emission scanning electron microscope JSM-7600F (SEM) equipped with an Inca Energy Detector and Pulse Processor (EDXS) (JEOL Ltd., Tokyo, Japan). The analyses were performed using an acceleration voltage of 15 kV. The digitalized microstructures were processed with the Image Tool software[14] to obtain the areas of more than 200 grains. The grain size was expressed as the Feret's diameter (d_F).

Prior to electrical characterization, gold/palladium electrodes were sputtered on samples cut in the form of disks and were polished. Typical dimensions of the samples were 6 mm in diameter and 0.6 mm in thickness. A bipolar triangular waveform was applied to the sample with a high voltage amplifier (Trek Model 20/20C, Trek Inc., Medina, NY) driven by a frequency generator (Agilent 33220A, Santa Clara, CA). The polarization and strain hysteresis loops were characterized at a frequency of 50 mHz and a maximum field of 3.5 kV/mm. Strain–electric field curves are plotted by setting the minimum strain to be zero. For small signal electrical measurements, each sample was poled at 160°C with 3 kV/mm for 15 min. The capacitance and loss factor, tan δ, were measured at 1 kHz using an HP 4192A LF Impedance Analyzer (Santa Clara, CA). The coupling coefficients, k_p, k_t, and quality factor, Q_m, were obtained using the resonance method (Bode, Klaus, Austria). The piezoelectric coefficient, d_{33}, was determined with a Berlincourt piezometer at 100 Hz (Take Control PM10, Birmingham, UK).

The frequency and stress field amplitude dependence of the piezoelectric d_{33} coefficient was measured by a Berlincourt-type d_{33} meter.[15]

III. Results and Discussion

(1) Density and Microstructure

To determine the effect of zirconia inclusions on the grain size of PZT matrix, the samples were analyzed by SEM using

backscattered electrons (BE). The SEM-BE micrographs of the thermally etched surfaces and fracture surfaces of PZT–xTZ composites show the lighter PZT matrix phase with dark-gray ZrO_2 inclusions and pores (Fig. 3). Zirconia is located along the grain boundaries and in the PZT grains; the coalescence of zirconia grains in the composites can be seen. The addition of zirconia to PZT hinders the matrix grain growth (Fig. 3, left column) and changes the fracture mode (Fig 3, right column). In Table I, the mean Ferret's diameters (d_F) of the matrix grain size in PZT–xTZ composites with the corresponding densities are given. The d_F of the matrix grain size is 3.3 (±1.6) μm and decreases with increasing zirconia content to 1.0 (±0.4) μm for PZT–20TZ. The estimated d_F value for zirconia grains in all composites was ~0.2 (±0.1) μm. The addition of TZ to PZT had no large impact on the density, that is, the densities of the composites were between 94.6% and 97.4% of TD.

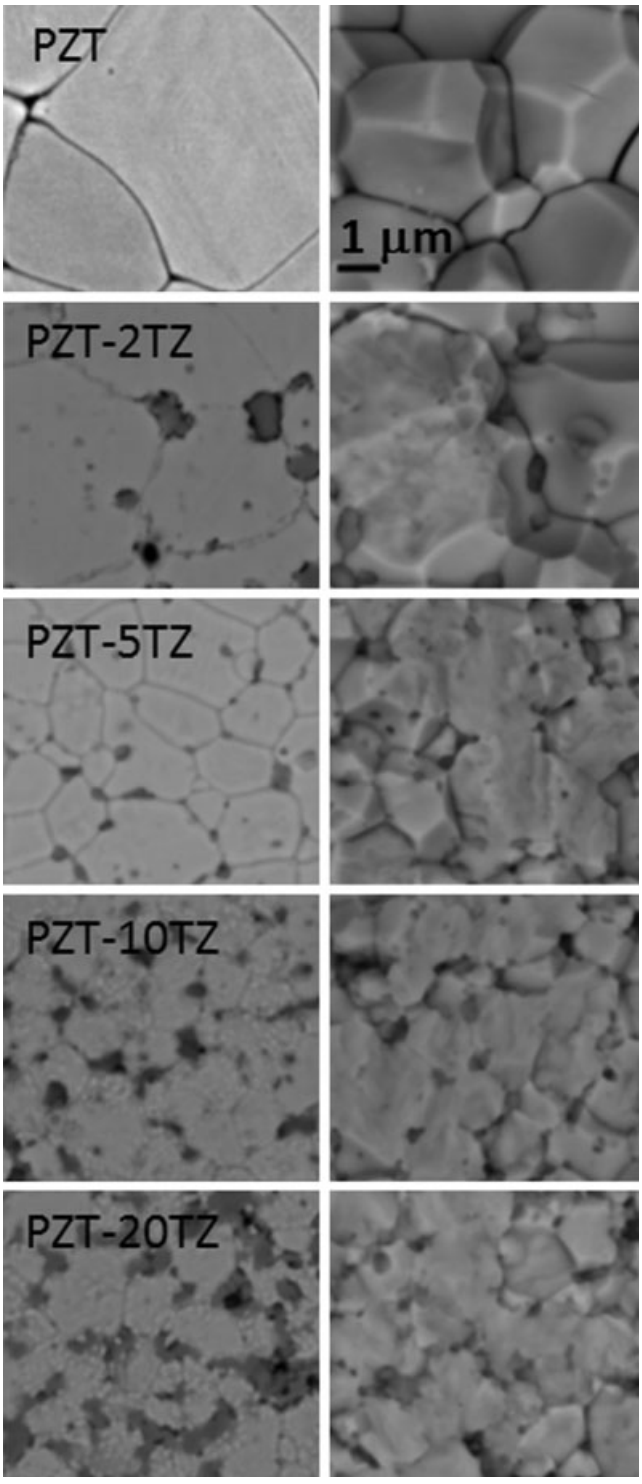

Fig. 3. SEM-BE images of thermally etched microstructures (left column) and fracture surfaces (right column) of PZT–xTZ composites, after sintering at 1275°C for 2 h. Dark, round inclusions are ZrO_2 grains. Images are presented at the same magnification.

The fracture surface of pure PZT is predominantly intergranular. However, as the zirconia content is increased, there is an increase in the ratio of trans-to-intergranular fracture. Similarly, it was observed that the addition of ZrO_2 into $K_{0.5}Na_{0.5}NbO_3$ (KNN) ceramics increased the ratio of trans-to-intergranular fracture and inhibited the matrix grain growth.[16] In this case, the reason for the decreased mobility of the matrix grain boundaries was ascribed to presence of ZrO_2 particles at the grain junctions and a limited solubility of Zr in the grain boundary region relative to KNN grain interior. However, due to the higher solubility of Zr in PZT, the mechanism of the grain growth inhibition related to the Zr limited solubility in the grain boundary region appears improbable.

(2) Phase Composition

The X-ray powder diffraction patterns of PZT–xTZ composites, sintered at 1275°C for 2 h are shown in Fig. 4. The peaks in pure PZT can be indexed with tetragonal (T) phase (ICSD 90699, SG:P4mm). If present, the amount of rhombohedral (R) phase in this sample is comparably low. With an increasing TZ concentration, the rhombohedral phase (ICSD 90700, SG:R3mH) is more visible and becomes the major phase with 10 and 20 vol% TZ content (see Table II). The peaks with low intensity between 28° and 30.5° correspond to monoclinic and tetragonal ZrO_2 phases. By SEM/EDXS analysis, a low solubility of Ti in ZrO_2 was observed, which is in accordance with the PbO–TiO_2–ZrO_2 phase diagram,[17] suggesting that the compositions are close to the thermodynamic equilibrium at the sintering temperature.

Table I. The Calculated d_F for PZT Matrix Grains in PZT–xTZ Composites Analyzed by ImageTool Program and Corresponding Densities

Material	d_F (±SD) for PZT grains (μm)	Density (%TD), g/cm^3
PZT	3.3 (±1.6)	7.70 (96.3)
PZT–2TZ	3.1 (±1.6)	7.53 (94.6)
PZT–5TZ	1.6 (±0.8)	7.64 (95.4)
PZT–10TZ	1.3 (±0.5)	7.58 (97.4)
PZT–20TZ	1.0 (±0.4)	7.28 (96.2)

TD, theoretical density.

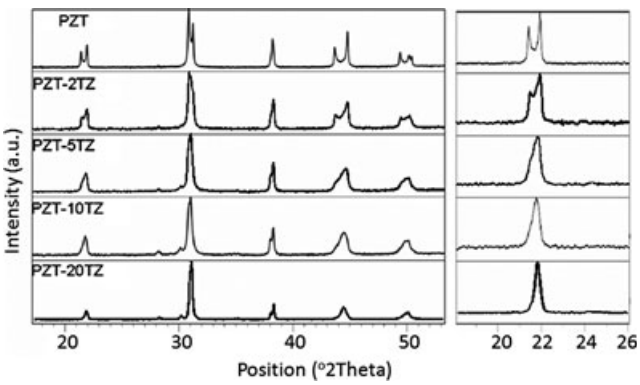

Fig. 4. XRD patterns of PZT–xTZ composites after sintering at 1275°C for 2 h. Right: first peaks, corresponding to the (100) family of tetragonal and the $(10\bar{2})$ reflection of the rhombohedral phase are shown.

Table II. Results of the Rietveld Refinement for PZT–*x*TZ Composites

Material	Tetragonal content (wt%) [$R_{w(all)}$, GOF]	V_T (Å^3)	Rhombohedral content (wt%) [$R_{w(all)}$, GOF]	V_R (Å^3)	V_R(/6) (Å^3)
PZT	~100 [5.24, 4.07]	67.61 (1)	–	–	–
PZT–2TZ	58 (1) [4.77, 2.20]	67.70 (1)	42 (1) [4.45, 2.20]	406.24 (3)	67.71
PZT–5TZ	34 (1) [4.20, 2.38]	67.70 (1)	66 (1) [3.92, 2.38]	406.35 (3)	67.72
PZT–10TZ	23 (1) [3.62, 2.30]	67.74 (2)	77 (1) [3.13, 2.30]	406.65 (4)	67.78
PZT–20TZ	17 (1) [4.61, 2.76]	67.79 (2)	83 (1) [4.22, 2.76]	406.80 (5)	67.80

The reduced volume (from $Z = 1$ to $Z = 6$) of the rhombohedral phase (V_R) is added for an easier comparison with the volume of the tetragonal phase (V_T) ($Z = 1$).The reliability factors $R_{w(all)}$ (%) and goodness of fit (GOF) are also added.

The results of the refinements are summarized in Table II. The amount of tetragonal phase decreases with the addition of TZ. The diffusion of zirconium into the perovskite PZT lattice is most likely the main factor responsible for the shift from the primarily tetragonal phase at low TZ content to a mixed phase system (rhombohedral/tetragonal) at higher TZ content. This is in agreement with the phase diagram of PZT, which shows that the zirconium-rich phases are rhombohedral.[17] Although the phase composition of PZT can also be affected by the addition of Y_2O_3,[18,19] the effects are assumed to be negligible due to the relatively small amount of yttrium in TZ. In addition to the changes in the relative amounts of T and R phases, there is also a gradual increase in the cell volume of these two phases with increasing zirconia content. This can also be a result of a small amount of zirconium replacing a part of titanium in the PZT cell. In fact, the radius of Zr^{4+} with the coordination number of 6 is 0.72 Å, compared to 0.605 Å for Ti^{4+} in the same configuration.[20]

In the following sections, the electrical and piezoelectric properties of PZT–*x*TZ composites are presented and explanations for observed behavior are given based on the previously presented microstructures and phase compositions.

(3) Dielectric Properties

The measurements of dielectric permittivity as a function of temperature (Fig. 5) revealed a broadening of the maximum permittivity with increasing TZ content in PZT, indicating perhaps a distribution of Curie temperatures (T_c) as composition varies throughout the sample. Interestingly, with a 2 vol% TZ addition to PZT, the T_c value was shifted toward lower temperature, that is, from ~360°C to 350°C. This was, however, not found with higher TZ concentrations, where T_c showed the opposite trend, that is, an increase up to 370°C. The observed changes in broadening and in shifts of T_c could be due to the changes in the phase composition (rhombohedral/tetragonal ratio) and in the matrix grain size as both vary with zirconia content. In the PZT phase diagram, the T_c monotonously decreases as Zr/Ti ratio is increased. Most probably, the major factor influencing the lowering of T_c for PZT–2TZ is the slight shift in composition and thus the crystal structure from tetragonal to rhombohedral (see Table II) and not a grain size effect, as there was only a small difference in the matrix grain size between PZT (3.3 μm) and PZT–2TZ (3.1 μm). More pronounced differences in the matrix grain size occurred at additions of zirconia greater than 2 vol%, where grain sizes of 1.6, 1.3, and 1 μm were found for PZT–5TZ, –10TZ, and –20TZ, respectively. In those cases, even though incorporation of Zr into the lattice changed the crystals structure from tetragonal to rhombohedral, the grain size effects may be the predominant factor influencing the shift of the ferroelectric-to-paraelectric phase transition toward higher temperatures. This can, for example, happen due to anisotropic internal stresses in the PZT matrix with small grain size. Martirena *et al.*[21] showed, for example, that with decreasing grain size in Nb-doped PZT, the T_c is shifted to higher values.

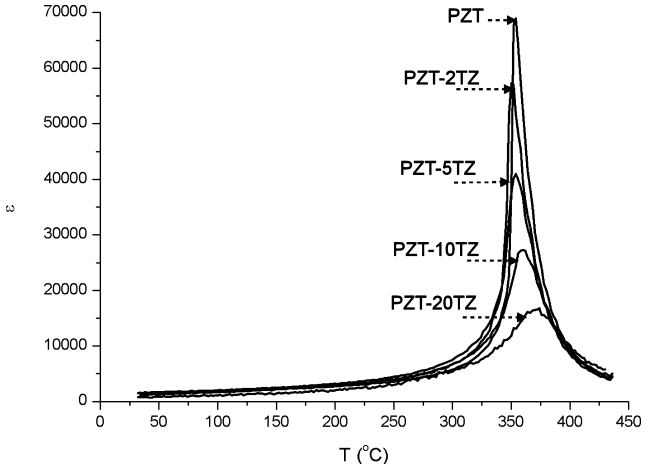

Fig. 5. Temperature dependence of dielectric permittivity for PZT–*x*TZ composites, measured at 1 kHz.

The room-temperature dielectric permittivity and dielectric losses of poled samples are shown in Table III. A nonlinear decrease in dielectric permittivity was observed in all materials containing zirconia particles. The 2 vol% addition of TZ, for example, decreased the dielectric permittivity by 15% (from 1810 to 1530), whereas zirconia concentrations of 20 vol% resulted in a permittivity decrease of 62% (from 1800 to 680). The dielectric losses, measured at 1 kHz, were found to be independent of zirconia concentration, with values for all samples between 0.02 and 0.03.

The comparable dielectric constant in pure PZT and PZT–2TZ could be related mainly to the change in phase composition from a nearly tetragonal structure to a mixed phase system (R and T). This observation is in accordance with the literature, where the highest dielectric constant was reported for a composition just on the tetragonal side of the MPB in the PZT phase diagram.[1] In the composites with 5 or more vol% TZ several parameters can simultaneously influence its dielectric properties. In addition to the phase composition (with addition of TZ to PZT, the R/T ratio is increased) and the grain size (with addition of TZ, the matrix grain size decreases from 3.1 μm for PZT–2TZ to 1.0 μm for PZT–20TZ), the dilution of ferroelectric PZT with dielectric TZ reduces the overall permittivity of the composites. For

Table III. The Dielectric and Piezoelectric Properties of Poled PZT–*x*TZ Composites

Material	ε 1 (kHz)	tan δ 1 (kHz)	d_{33} (pC/N)	k_p (/)	k_t (/)	Q_m (/)
PZT	1809	0.02	505	0.71	0.52	50
PZT–2TZ	1532	0.02	475	0.62	0.46	57
PZT–5TZ	1173	0.02	395	0.58	0.42	69
PZT–10TZ	1153	0.02	311	0.53	0.45	89
PZT–20TZ	678	0.03	157	0.34	0.34	140

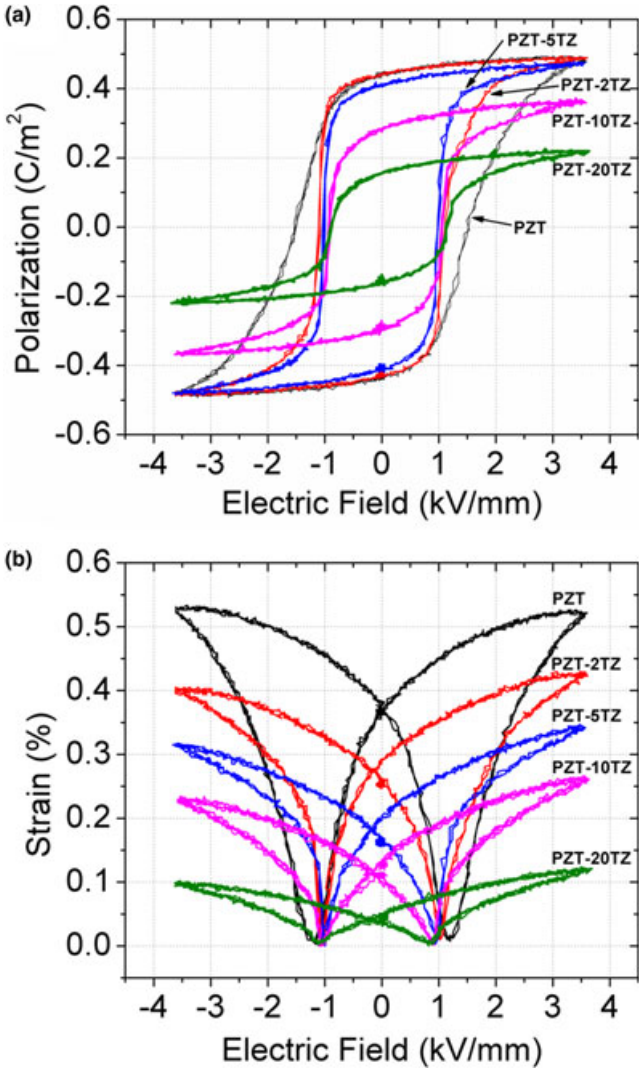

Fig. 6. Polarization (a)—and strain (b)—electric field hysteresis loops for PZT–*x*TZ composites, measured with a maximum electric field of 35 kV/mm at 50 mHz.

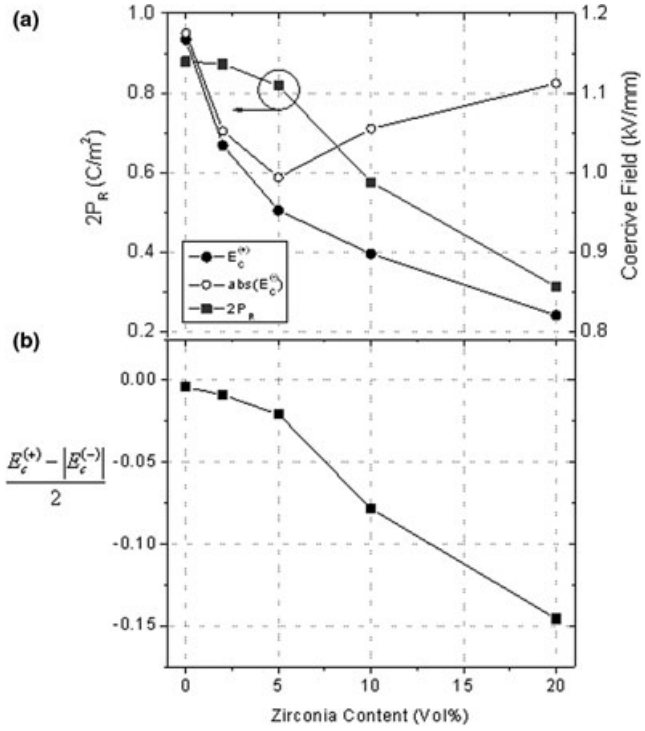

Fig. 7. Remanent polarization and coercive field ($E_c^{(+)}$ and $E_c^{(-)}$), as a function of zirconia content (a). Internal bias field as a function of zirconia content (b).

example, according to the spherical inclusions model for ferroelectric–dielectric composites,[22] the addition of 20 vol% of TZ to PZT would theoretically lower the permittivity of PZT by ~30%.

(4) Ferroelectric and Strain–Electric Field Hysteresis Loops

Figures 6(a) and (b) shows the polarization (P–E) and strain (S–E) hysteresis loops for PZT–*x*TZ composites, measured during bipolar electrical cycling at 50 mHz with a maximum electric field of 3.5 kV/mm. With increasing zirconia content, there is a decrease in remanent polarization, P_R, and coercive field, E_c, [Fig. 6(a)] as well as a corresponding change in the overall shape of the polarization hysteresis. The remnant polarization $2P_R$, which decreased from 0.88 for PZT to 0.32 C/m^2 for PZT–20TZ, changed considerably only for TZ content of 10% and 20%, whereas the coercive field decreased rapidly at low zirconia levels [Fig. 7(a)]. The change of coercive field, however, was found to be asymmetrical. Interestingly, pure PZT displayed a more gradual polarization reorientation during ferroelectric switching, whereas with the addition of 2, 5, 10, and 20 vol% zirconia, the hysteresis loops became considerably more squared.

It is apparent that the largest observed coercive field E_c was found for pure PZT, that is, the composition just on the tetragonal side of the MPB.[23] With increasing TZ content, however, there is an increasing asymmetry in both the P–E and S–E hysteresis, similar to that observed in hard PZT.[24] This resulted in asymmetrical changes of both the coercive field (Fig. 7) and the maximum strain [Fig. 6(b)], which was not observed in pure PZT. A decrease in E_c with increasing TZ content was found on the side of the butterfly loop with the highest strain, labeled herein as $E_c^{(+)}$. On the side with a lower maximum strain, however, there is an initial decrease in E_c, labeled herein as $E_c^{(-)}$, up to 5 vol%, above which the coercive field increased.

A number of factors can influence the coercive field value of PZT, including composition,[25] grain size,[26] and measurement frequency.[27,28] With increasing zirconia content, a shift in PZT composition toward the zirconia-enriched rhombohedral phase and a decrease in grain size were both observed. An increase in rhombohedral phase has been shown to decrease E_c, whereas a decrease in grain size leads to an increase of E_c due to the clamping of the domains.[29] Interestingly, in the PZT–*x*TZ composites both an increase and a decrease in the coercive field were observed dependent on, which direction of the field the maximum strain was found. In fact, it is found that the internal bias field $\frac{1}{2}\left(E_c^{(+)} - \left|E_c^{(-)}\right|\right)$ actually increases with increasing zirconia content [Fig. 7(b)]. This indicates that while E_c is decreasing, there is an increasing internal negative bias, which gives the impression that coercive field is increasing on one side and decreasing on the other side. This can be explained by preferential pinning in one direction of field by the hard zirconia particles, which are hard inclusions within a softer matrix, making the material appear like a hard-doped PZT. Alternatively, in analogy to Fe^{3+}-doped (hard) PZT, the hardening effect could also be explained by the incorporation of Y^{3+} on the B-site of the PZT lattice, although this is less probable because of the large Y^{3+} ionic radius (0.99 A) in comparison to Zr^{4+} (0.72 A) and Ti^{4+} (0.605 A). Indeed, the available literature data assumed Y^{3+} as A-side donor dopant in PZT.[18]

Similar to E_c, the highest $2P_R$ value was observed for pure PZT ($2P_R$ = 88 C/m^2), although only a minor decrease was

found ($2P_R$ = 87 C/m^2) for PZT–2TZ. Interestingly, at lower maximum applied electric field levels (not shown), it was observed that PZT–2TZ displayed the largest remanent polarization, indicating that zirconia concentrations at this level can assist polarization switching. According to Jaffe *et al.*,[1] the maximum remanent polarization occurs in a rhombohedral composition. With further addition (5, 10, or 20 vol%) of TZ into PZT, a more substantial decrease in P_R and in maximum strain was detected. This decrease in electromechanical properties can be related to the observed reduction in grain size,[30] the change in phase composition,[1] and the increasing reduction in the volume fraction of electrically active material.

(5) Piezoelectric Properties

In Table 3, the piezoelectric properties of PZT and the PZT–xTZ composites are presented. The PZT–xTZ composites were found to display a lower piezoelectric constant, d_{33}, as well as lower coupling factors, k_p and k_t, compared to the ceramics without zirconia. The d_{33} was found to decrease from 505 to 157 pC/N, k_p from 0.71 to 0.34, and k_t from 0.52 to 0.34 as zirconia concentration increased to 20 vol%. The Q_m factor increased from 50 for PZT to 140 for PZT–20TZ.

In analogy to the dielectric properties of PZT–xTZ, the decrease of d_{33} and coupling factors can be related to the observed changes in phase composition, the grain size, and the dielectric/piezoelectric (TZ/PZT) ratio in the composites. The results are in accordance with the literature; Jaffe *et al.*[1] showed that the highest values for d_{33} and coupling factors can be obtained for the ceramics with a composition just on the tetragonal side of the MPB, that is, in our study, this is pure PZT. The decrease of d_{33}, k_p, and k_t values in the composites can be also related to the reduction in grain size as explained by Randall *et al.*[30] In fact, the authors reported that the decrease in grain size in the range of 0.1–10 μm leads to the reduction of piezoelectric coefficients of $Pb_{0.98}(Zr_{0.52}Ti_{0.48})_{0.92}Nb_{0.0004}O_3$ ceramics, presumably due to reduced number of domain variants, that is, simple domain configuration.

Due to the difference in the piezoelectric and dielectric properties of the individual components in the composite, Maxwell–Wagner piezoelectric effects could arise, leading to frequency dependence of the piezoelectric coefficients.[31] In addition, TZ could also indirectly affect the extrinsic (domain-wall) contribution to the piezoelectric response, for example, through change of phase composition and/or grain size. These possibilities were investigated by measuring the d_{33} coefficient of the pure PZT and the composite ceramics as a function of frequency and amplitude of the alternating stress field.

Figure 8 provides the frequency dependence of the piezoelectric d_{33} coefficient of pure PZT and PZT–xTZ composites. All the samples show an increase of the d_{33} coefficient with decreasing frequency, as usually observed for soft PZT compositions.[32,33] A considerable reduction of the d_{33} in the whole frequency range is observed upon the addition of TZ. Also, note that with increasing TZ content, the d_{33} becomes less frequency dependent, that is, the slope of the linear d_{33} versus log-frequency relationship is gradually decreasing with increasing TZ content.

In addition to the frequency dependence, the influence of the AC stress amplitude on the d_{33} was also measured. Figure 9 displays the piezoelectric d_{33} coefficient as a function of the stress amplitude at 1 Hz. In all the cases, the d_{33} increases in a closely linear fashion with increasing stress amplitude. Such behavior is typically observed in soft PZT and is related to the extrinsic (non-180° domain wall) contribution to the piezoelectric coefficient, that is, the non-180° domain walls, which behave both as elastic and electric dipoles and are particularly mobile in soft PZT, will move under external AC stress field, giving a large contribution to the piezoelectric response. In fact, in the case of pure PZT, with the composition close to the MPB, the total increase in the piezoelectric response with stress, that is, from 0.2 to 5 MPa peak-to-peak, is 33%. This nonlinear behavior is gradually diminishing in proportion to the amount of TZ added into the PZT; the lowest relative increase in d_{33} with stress amplitude (19%) is that of the sample with 20% of TZ.

In comparison with pure PZT, the reduced frequency dispersion (Fig. 8) coupled with the reduced nonlinearity (Fig. 9) with TZ additions suggest a minor extrinsic (non-180° domain wall) contribution in these samples. One of the possibilities of the origin of the decreased extrinsic contribution in PZT–TZ composites, as compared to pure PZT, is the shift of the composition away from the MPB due to TZ addition. To test this hypothesis, we performed measurements on a pure PZT specimen with the nominal Zr/Ti ratio 55/45, that is, exhibiting the predominant rhombohedral phase similar to that in PZT–20TZ (see Fig. 4 and Table 2). Even if close in phase composition, 55/45 PZT and PZT–20TZ showed quantitatively very different frequency and

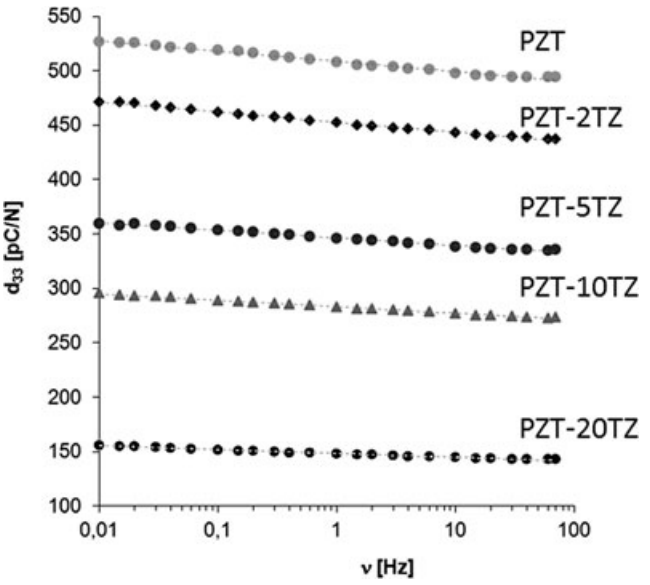

Fig. 8. Piezoelectric d_{33} coefficient as a function of frequency for PZT and for PZT–xTZ composites. The dashed lines are guide for the eye (peak-to-peak stress 2 MPa).

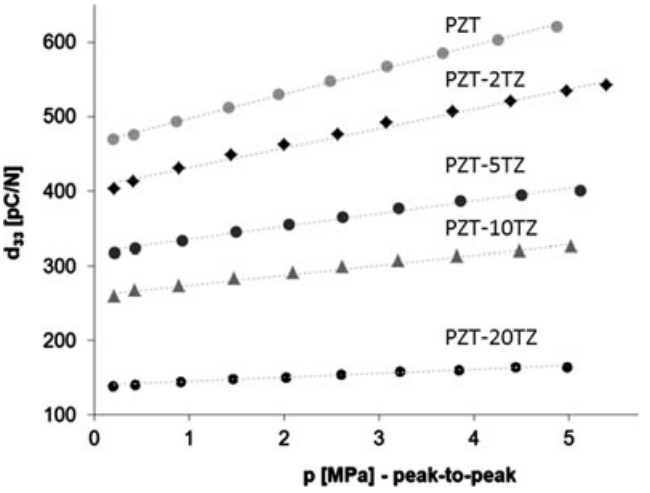

Fig. 9. Piezoelectric d_{33} coefficient as a function of the stress amplitude for PZT and PZT–xTZ composites (at frequency of 1 Hz and at a static pressure of 12.5 MPa). The dashed lines are guide for the eye.

stress dependence of d_{33} (results are not shown). In comparison with PZT–20TZ, the PZT55/45 ceramics exhibited both larger d_{33} at the lowest measured stress, that is, 210 pC/N at 0.2 MPa, and a much larger relative increase in d_{33} with stress (80%). This suggests that the decreased extrinsic contribution in TZ-added PZT cannot be explained by the shift in the composition away from MPB; hence, other influences are important, such as the reduced grain size and the dielectric/piezoelectric (TZ/PZT) ratio. For example, it was experimentally shown for $BaTiO_3$ that the activity of domain walls is considerably reduced in fine-grained (below 1 μm) ceramics; this was manifested as a smaller increase of d_{33} by stress in fine-grained ceramics in comparison with the coarse-grained ceramics.[34]

IV. Summary

The PZT $[Pb_{0.98}Ba_{0.01}][(Zr_{0.53}Ti_{0.47})_{0.98}Nb_{0.02}]O_3$ with varying concentrations (2, 5, 10, and 20 vol%) of yttria-stabilized zirconia (TZ) was prepared by solid-state synthesis to study the effect of zirconia on the microstructure and the electrical properties. We suggest that zirconium diffuses into the PZT, which resulted in a shift of the matrix phase composition toward the zirconia-rich rhombohedral phase. This resulted in an increase in the R/T ratio in comparison to the original matrix phase. The addition of zirconia hinders the matrix grain growth and changes the fracture mode. Lower dielectric and piezoelectric properties of PZT–*x*TZ composites can be related to the observed changes in phase composition, the grain size, and dielectric/piezoelectric (TZ/PZT) ratio. Polarization and strain hysteresis loops measurements indicated that the zirconia particles in PZT acts as pinning centers for ferroelectric domain switching. In addition, the reduced frequency dispersion and the reduced nonlinearity of the piezoelectric d_{33} coefficient in PZT–*x*TZ composites also suggest minor extrinsic contributions in these samples.

Acknowledgment

The authors thank Ms. Jena Cilenšek and Mitja Kamplet for support in the experimental work.

References

[1]B. Jaffe, W. R. Cook, and H. Jaffe, "Solid Solutions of Pb(Ti,Zr,Sn,Hf) O_3"; pp. 135–70 in *Piezoelectric Ceramics*, Edited by. J. P. Roberts and P. Popper. Academic Press, London, 1971.

[2]C. A. Randall, A. Kelnberger, G. Y. Yang, R. E. Eitel, and T. R. Shrout, "High Strain Piezoelectric Multilayer Actuators – A Material Science and Engineering Challenge," *J. Electroceram.*, **14**, 177–91 (2005).

[3]T. Yamamoto, H. Igarashi, and K. Okazaki, "Electrical and Mechanical Properties of SiC Whisker Reinforced PZT Ceramics," *Ferroelectrics*, **63**, 281–8 (1985).

[4]H. B. Lin, M. S. Cao, Q. L. Zhao, X. L. Shi, D. W. Wang, and F. C. Wang, "Mechanical Reinforcement and Piezoelectric Properties of Nanocomposites Embedded with ZnO Nanowhiskers," *Scripta Mater.*, **59**, 780–3 (2008).

[5]B. Malič, M. Kosec, and T. Kosmac, "Mechanical and Electric Properties of PZT-ZrO_2 Composites," *Ferroelecrics*, **129**, 147–55 (1992).

[6]K. Tajima, H. J. Hwang, M. Sando, and K. Niihara, "PZT Nanocomposites Reinforced by Small Amount of Oxides," *J. Eur. Ceram. Soc.*, **19**, 1179–82 (1999).

[7]Y. Wu and T. Feng, "Fabrication and Mechanical Reinforcement of Piezoelectric Nanocomposites with ZrO_2 Nanoparticles Embedded In Situ," *J. Alloys Compd.*, **491**, 452–5 (2010).

[8]B. W. Chua, L. Lu, M. O. Lai, and G. H. L. Wong, "Effects of Complex Additives on Toughness and Electrical Properties of PZT Ceramics," *J. Alloys Compd.*, **381**, 272–7 (2004).

[9]A. G. Evans and R. M. Cannon, "Toughening of Brittle Solids by Martensitic Transformations," *Acta Metall.*, **34** [5] 761–800 (1986).

[10]R. H. Hannink, P. M. Kelly, and B. C. Muddle, "Transformation Toughening in Zirconia-Containing Ceramics," *J. Am. Ceram. Soc.*, **83** [3] 461–87 (2000).

[11]L. Gmelin, *Handbuch der Anorganischen Chemie (Handbook of Anorganic Chemistry)*, Universitäts-Buchhandlung von Karl Winter, Heidelberg, 1853.

[12]R. B. Atkin and R. M. Fulrath, "Point Defects and Sintering of Lead Zirconate-Titanate," *J. Am. Ceram. Soc.*, **54** [5] 265–70 (1971).

[13]V. Petricek and M. Dusek, *The Crystallographic Computing System JANA 2000*, Institute of Physics, Prague, Czech Republic, 2006.

[14]Image Tool 3.00, Don Wilcox, Brent Dove, Doss McDavid, David Greer, The University of Texas Health Science Center, USA. 2002.

[15]A. Barzegar, D. Damjanovic, and N. Setter, "The Effect of Boundary Conditions and Sample Aspect Ratio on Apparent d_{33} Piezoelectric Coefficient Determined by Direct Quasistatic Method," *IEEE Trans. UFFC*, **51**, 262–70 (2004).

[16]B. Malic, J. Bernard, A. Bencan, and M. Kosec, "Influence of Zirconia Addition on the Microstructure of $K_{0.5}Na_{0.5}NbO_3$ Ceramics," *J. Eur. Ceram. Soc.*, **28**, 1191–6 (2008).

[17]A. H. Webster, R. C. MacDonald, and W. S. Bowman, "The System PbO-ZrO_2-TiO_2 at 1100°C," *J. Can. Ceram. Soc.*, **34**, 97–102 (1965).

[18]A. Beitollahi and C. H. Khezri, "Effect of the Addition of Y_2O_3 on the Structure, Microstructure and Piezoelectric Properties of PZT(53/47)," *J. Mater. Sci. Mater. Electron.*, **12**, 707–14 (2001).

[19]R. F. Zhang, H. P. Zhang, J. Ma, Y. Z. Chen, and T. S. Zhang, "Effect of Y and Nb Codoping on the Microstructure and Electrical Properties of Lead Zirconate Titanate Ceramics," *Solid State Ionics*, **166**, 219–23 (2004).

[20]R. D. Shannon, "Revised Effective Ionic-Radii and Systematic Studies of Interatomic Distances in Halides and Chalcogenides," *Acta Crystallogr. Sect. A*, **32**, 751–67 (1976).

[21]H. T. Martirena and J. C. Burfoot, "Grain-Size Effects on Properties of Some Ferroelectric Ceramics," *J. Phys. C: Solid State Phys.*, **7**, 3182–92 (1974).

[22]V. O. Sherman, A. K. Tagantsev, N. Setter, D. Iddles, and T. Price, "Ferroelectric-Dielectric Tunable Composites," *J. Appl. Phys.*, **99**, 074104-10 (2006).

[23]D. C. Lupascu. "The Lead-Zirconate-Titanate Crystal System"; pp. 12. in *Fatigue of Ferroelectric Ceramics and Related Issues*, Edited by R. Hull, R.M. Osgood, J. Parisi, and H. Warlimont. Springer, Heidelberg, 2004.

[24]T. Ogawa and K. Nakamura, "Bipolar Pulse Poling and Space Charge Field in Lead Zirconate Titanate Ceramics," *J. Eur. Ceram. Soc.*, **21**, 1391–4 (2001).

[25]H. Kungl, R. Theissmann, M. Knapp, C. Baehtz, H. Fuess, S. Wagner, T. Fett, and M. J. Hoffmann, "Estimation of Strain From Piezoelectric Effect and Domain Switching in Morphotropic PZT by Combined Analysis of Macroscopic Strain Measurements and Synchrotron X-ray Data," *Acta Mater.*, **55** [6] 1849–61 (2007).

[26]M. J. Hoffmann, M. Hammer, A. Endriss, and D. C. Lupascu, "Correlation Between Microstructure, Strain Behavior, and Acoustic Emission of Soft PZT Ceramics," *Acta Mater.*, **49** [7] 1301–10 (2001).

[27]A. Picinin, M. H. Lente, J. A. Eiras, and J. P. Rino, "Theoretical and Experimental Investigations of Polarization Switching in Ferroelectric Materials," *Phys. Rev. B*, **69** [6] 0641171-8 (2004).

[28]T. Liu and C. S. Lynch, "Orientation Dependence of Nonlinearity and Hysteresis in PZN-4.5%PT Single Crystals II: Bipolar Electromechanical Response," *J. Intell. Mater. Syst. Struct.*, **17**, 931–7 (2006).

[29]C. Sakaki, B. L. Newalkar, S. Komarneni, and K. Uchino, "Grain Size Dependence of High Power Piezoelectric Characteristics in Nb Doped Lead Zirconate Titanate Oxide Ceramics," *Jpn. J. Appl. Phys., Part 1*, **40** [12] 6907–10 (2001).

[30]C. A. Randall CA, N. Kim, J. P. Kucera, W. W. Cao, and T. R. Shrout, "Intrinsic and Extrinsic Size Effects in Fine-Grained Morphotropic-Phase-Boundary Lead Zirconate Titanate Ceramics," *J. Am. Ceram. Soc.*, **81** [3] 677–88 (1998).

[31]D. Damjanovic, M. D. Maeder, P. D. Martin, C. Voisard, and N. Setter, "Maxwell-Wagner Piezoelectric Relaxation in Ferroelectric Heterostructures," *J. Appl. Phys.*, **90** [11] 5708–12 (2001).

[32]D. Damjanovic, M. Demartin, H. S. Shulman, M. Testorf, and N. Setter, "Instabilities in the Piezoelectric Properties of Ferroelectric Ceramics," *Sens. Act.*, **A53** [1–3] 353–60 (1996).

[33]D. Damjanovic, S. S. N. Bharadwaja, and N. Setter, "Toward Unified Description of Nonlinearity and Frequency Dispersion of Piezoelectric and Dielectric Responses in $Pb(Zr,Ti)O_3$," *Mater. Sci. Eng.*, **B 120**, 170–4 (2005).

[34]M. Demartin and D. Damjanovic, "Dependance of the Direct Piezoelectric Effect in Coarse and Fine Grain Barium Titanate Ceramics on Dynamic and Static Pressure," *Appl. Phys. Lett.*, **68** [21] 3046–8 (1996). □